PERGAMON

International Journal of Solids and Structures 39 (2002) 4395–4406

INTERNATIONAL JOURNAL OF SOLIDS and STRUCTURES

www.elsevier.com/locate/ijsolstr

Moving eccentric crack in a piezoelectric strip bonded to elastic half planes

Soon Man Kwon [a], Jung Seek Lee [b], Kang Yong Lee [b,*]

[a] *School of Mechanical Engineering, Yeungnam University, 214-1, Daedong, Kyongsan, Kyongbuk 712-749, South Korea*
[b] *School of Mechanical Engineering, College of Engineering, Yonsei University, Seoul 120-749, South Korea*

Received 6 January 2002; received in revised form 2 May 2002

Abstract

We consider the problem of determining the singular stresses and electric fields in a piezoelectric ceramic strip which contains an eccentric crack moving at constant speed. The strip is sandwiched between two elastic half planes under combined anti-plane mechanical shear and in-plane electrical loadings. The analysis is conducted on the *permeable crack condition* by the integral transform approach. The field intensity factors and energy release rate are obtained in terms of a Fredholm integral equation of the second kind. Some numerical results for the dynamic stress intensity factor and the dynamic energy release rate are presented graphically to show the effects of the crack propagation speed as well as the electromechanical coupling coefficient. The initial crack branch angle for a PZT-5H piezoceramic structure is also predicted by maximum energy release rate criterion.
© 2002 Elsevier Science Ltd. All rights reserved.

Keywords: Moving eccentric crack; Piezoelectric material; Field intensity factors; Crack branch; Electromechanical coupling coefficient

1. Introduction

Because of the coupling characteristics between electric and mechanical deformation, piezoelectric materials have been widely used in many engineering applications. Due to the intrinsic brittle property, however, the stress concentration caused by mechanical and/or electric load may induce the initiation and propagation of a crack. Also, the original defects embedded in ceramic, such as voids, inclusions and cracks, have dominant influence on the failure of structure components. To judge whether the material with defects continues to be used safely, it is requisite to understand damage and fracture behavior of piezoceramic materials.

The increasing attention to the study of crack problems in piezoelectric materials in the last decade has led to a lot of significant works. Especially, the influence of the crack moving speed on the crack tip field was a popular subject in classical elastodynamics. However, relatively less attention is given to

* Corresponding author. Tel./fax: +82-2-2123-2813.
E-mail addresses: soonmankwon@hanmail.net (S.M. Kwon), fracture@yonsei.ac.kr (K.Y. Lee).

0020-7683/02/$ - see front matter © 2002 Elsevier Science Ltd. All rights reserved.
PII: S0020-7683(02)00338-4

elastodynamical moving crack problem in piezoelectric materials. Yoffe (1951) considered the problem of a crack of fixed length at constant speed through a stretched isotropic solid of infinite extent. Based on the criterion of maximum circumferential stress ahead of the crack tip, she concluded that there is a critical velocity of about 0.6 times the shear wave velocity at which the *crack tends to curve and branch out*, while at lower velocities, the initial growth is expected to occur along the line of the crack. By considering this problem for a piezoelectric medium, it is the purpose of this investigation to find out the influence of electromechanical interaction on the initial propagation direction of a crack moving at constant speed.

The Yoffe crack problem in a piezoelectric material was first investigated by Chen and Yu (1997). The result implied that the moving speed of the crack had no influence on the intensities of the stress and electric displacement. Recently, Chen et al. (1998) studied an interface Yoffe crack problem, and showed that the stress and electric displacement intensity factors are dependent on the crack speed. But, the above Yoffe crack researches have drawbacks. The impermeable boundary condition on the crack surface was used. With this condition enforced, the electric displacement intensity factor depends on the electric load, and the energy release rate is always negative in the presence of electric loading only, irrespective of its sign. This contradicts available experimental observations (Tobin and Pak, 1993; Park and Sun, 1995a,b) in reality, the crack may have some small electrical conductivity. Thus, the zero charge equation of electrostatics in the impermeable crack boundary condition must be replaced by the equation of the continuity of electric charge (Jackson, 1976). In fact, cracks in piezoelectric media will be filled with vacuum or air; both the components of electric displacement and the electric field will be continuous across the crack faces.

In this paper, we consider the problem for the Yoffe-type moving eccentric crack in an infinitely long piezoelectric ceramic strip sandwiched between elastic half planes under an exact permeable crack condition and the combined anti-plane mechanical shear and in-plane electrical loadings. The two elastic half planes have the same properties. By using integral transform techniques, the problem is reduced to the solution of a Fredholm integral equation of the second kind, which is obtained from two pairs of dual integral equations. Some numerical results for the dynamic stress intensity factor (DSIF) and the dynamic energy release rate (DERR) are presented graphically to show the effects of the crack propagation speed as well as the electromechanical coupling coefficient (EMCC). The initial crack branch angle for a PZT-5H piezoceramic structure is also predicted by maximum energy release rate criterion.

2. Problem statement and method of solution

The situation envisaged is that of an eccentric crack of length $2a$ propagating at constant speed v in an infinitely long piezoelectric strip sandwiched between two elastic half planes, which is subjected to the combined mechanical and electric loads as shown in Fig. 1. A set of Cartesian coordinates (X, Y, Z) is attached to the center of the crack for reference purposes. The piezoelectric ceramic strip poled with Z-axis occupies the region $(-\infty < X < \infty, -h_2 \leqslant Y \leqslant h_1, 2h = h_1 + h_2)$, and is thick enough in the Z-direction to allow a state of anti-plane shear. The uniform far-field shear stress, τ_∞, and uniform electric displacement, D_0 are applied. For convenience, we assume that the piezoelectric strip consists of upper ($Y \geqslant 0$, thickness h_1) and lower ($Y \leqslant 0$, thickness h_2) regions.

The electroelastic boundary value problem is simplified under the out-of-plane displacement and the in-plane electric fields in the forms,

$$u_{Xi} = u_{Yi} = 0, \quad u_{Zi} = w_i(X, Y, t), \tag{1}$$

$$E_{Xi} = E_{Xi}(X, Y, t), \quad E_{Yi} = E_{yi}(X, Y, t), \quad E_{Zi} = 0, \tag{2}$$

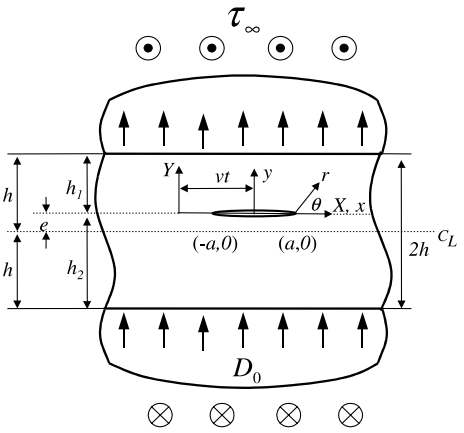

Fig. 1. A piezoelectric ceramic strip with an eccentric moving crack bonded to elastic half planes: definition of geometry and loading.

$$u_{Xi}^{\mathrm{E}} = u_{Yi}^{\mathrm{E}} = 0, \quad u_{Zi}^{\mathrm{E}} = w_i^{\mathrm{E}}(X, Y, t), \tag{3}$$

where u_{ki} and E_{ki} $(k = X, Y, Z)$ are displacements and electric fields, respectively. Subscript i $(i = 1, 2)$ stand for upper and lower regions, respectively, and superscript E represents elastic half planes.

For the current problem, it is convenient to introduce the following Galilean transformation

$$x = X - vt, \quad y = Y, \tag{4}$$

where (x, y) is the translating coordinate system attached to the moving crack. It is, however, assumed that the propagation of the ensuing crack has prevailed for such a long time that the stress distribution around its tip is time invariant in the translating reference frame.

Accordingly, the dynamic anti-plane governing equations for the piezoelectric and elastic materials can be written in terms of the moving coordinate system as

$$\alpha^2 \frac{\partial^2 w_i(x,y)}{\partial x^2} + \frac{\partial^2 w_i(x,y)}{\partial y^2} = 0, \quad \alpha \leqslant 1, \tag{5}$$

$$\beta^2 \frac{\partial^2 w_i^{\mathrm{E}}(x,y)}{\partial x^2} + \frac{\partial^2 w_i^{\mathrm{E}}(x,y)}{\partial y^2} = 0, \quad \beta \leqslant 1, \tag{6}$$

$$\nabla^2 \psi_i(x,y) = 0, \tag{7}$$

where

$$\alpha \equiv \sqrt{1 - (v/C_{\mathrm{T}})^2}, \quad \beta \equiv \sqrt{1 - (v/C_{\mathrm{T}}^{\mathrm{E}})^2}, \quad \psi_i \equiv \phi_i - e_{15} w_i / d_{11}, \quad C_{\mathrm{T}} = \sqrt{\mu/\rho}, \quad C_{\mathrm{T}}^{\mathrm{E}} = \sqrt{c_{44}^{\mathrm{E}}/\rho^{\mathrm{E}}},$$
$$\mu = c_{44} + e_{15}^2/d_{11}, \tag{8}$$

and c_{44}, d_{11}, e_{15}, ϕ_i, and c_{44}^{E} are the elastic shear modulus measured in a constant electric field, the dielectric permittivity measured at a constant strain, the piezoelectric constant, the electric potential, and the shear modulus of elastic half planes, respectively. Also, ψ_i, C_{T}, $C_{\mathrm{T}}^{\mathrm{E}}$, μ, ρ, and ρ^{E} are the Bleustein function (Bleustein, 1968), the speed of the piezoelectrically stiffened bulk shear wave, the shear wave velocity of the elastic material, the piezoelectrically stiffened elastic constant, the piezoelectric material density, and the elastic material density, respectively.

In terms of the independent variables w_i and ψ_i, the constitutive relations can be written as follows:

$$\tau_{kzi} = \mu w_{i,k} + e_{15}\psi_{i,k}, \quad D_{ki} = -d_{11}\psi_{i,k}, \quad \tau^{E}_{kzi} = c^{E}_{44} w^{E}_{i,k}, \tag{9}$$

where τ_{kzi} and D_{ki} $(k = x, y)$ are the stress and electric displacement components, respectively.

Owing to the symmetry in geometry and loading, it is sufficient to consider only the right side of the plane. The electroelastic boundary conditions under the exact permeable crack model can be stated below:

$$\tau_{yzi}(x, 0) = 0, \quad 0 \leqslant x < a, \tag{10}$$

$$w_1(x, 0) = w_2(x, 0), \quad a \leqslant x < \infty, \tag{11}$$

$$D_{y1}(x, 0^+) = D_{y2}(x, 0^-), \quad 0 \leqslant x < a, \tag{12}$$

$$E_{x1}(x, 0^+) = E_{x2}(x, 0^-), \quad 0 \leqslant x < a, \tag{13}$$

$$\phi_1(x, 0) = \phi_2(x, 0), \quad a \leqslant x < \infty, \tag{14}$$

$$\tau_{yz1}(x, 0) = \tau_{yz2}(x, 0), \quad a \leqslant x < \infty, \tag{15}$$

$$D_{y1}(x, 0) = D_{y2}(x, 0), \quad a \leqslant x < \infty, \tag{16}$$

$$\tau_{yz1}(x, h_1) = \tau^{E}_{yz1}(x, h_1), \tag{17}$$

$$\tau_{yz2}(x, -h_2) = \tau^{E}_{yz2}(x, -h_2), \tag{18}$$

$$w_1(x, h_1) = w^{E}_{1}(x, h_1), \tag{19}$$

$$w_2(x, -h_2) = w^{E}_{2}(x, -h_2), \tag{20}$$

$$\tau^{E}_{yz1}(x, +\infty) = \tau^{E}_{yz2}(x, -\infty) = \tau_{\infty}, \tag{21}$$

$$D_{y1}(x, h_1) = D_{y2}(x, -h_2) = D_0. \tag{22}$$

Applying Fourier cosine transforms to Eqs. (5)–(7), we can obtain the results as follows:

$$w_i(x, y) = \frac{2}{\pi}\int_0^{\infty} [A_{1i}(s)e^{s\alpha y} + A_{2i}(s)e^{-s\alpha y}]\cos(sx)\,ds + a_0 y, \tag{23}$$

$$\psi_i(x, y) = \frac{2}{\pi}\int_0^{\infty} [B_{1i}(s)e^{sy} + B_{2i}(s)e^{-sy}]\cos(sx)\,ds - b_0 y, \tag{24}$$

$$w^{E}_{1}(x, y) = \frac{2}{\pi}\int_0^{\infty} C_1(s)e^{-s\beta y}\cos(sx)\,ds + c_0 y + d_{01}, \tag{25}$$

$$w^{E}_{2}(x, y) = \frac{2}{\pi}\int_0^{\infty} C_2(s)e^{s\beta y}\cos(sx)\,ds + c_0 y + d_{02}, \tag{26}$$

where $A_{ji}(s)$, $B_{ji}(s)$, and $C_i(s)$ $(i, j = 1, 2)$ are the unknown functions to be determined from the given boundary conditions. a_0, b_0, c_0, and d_{0i} $(i = 1, 2)$ are real constants, which will be determined from the far field and interface loading conditions.

The corresponding stress, electric displacement, electric potential and electric field components are obtained in the forms

$$\tau_{yzi}(x,y) = \frac{2}{\pi}\int_0^\infty s[\mu\alpha A_{1i}(s)e^{s\alpha y} - \mu\alpha A_{2i}(s)e^{-s\alpha y} + e_{15}B_{1i}(s)e^{sy} - e_{15}B_{2i}(s)e^{-sy}]\cos(sx)\,ds + \mu a_0 - e_{15}b_0, \tag{27}$$

$$\tau^{E}_{yz1}(x,y) = -\frac{2c^{E}_{44}\beta}{\pi}\int_0^\infty sC_1(s)e^{-s\beta y}\cos(sx)\,ds + c^{E}_{44}c_0, \tag{28}$$

$$\tau^{E}_{yz2}(x,y) = \frac{2c^{E}_{44}\beta}{\pi}\int_0^\infty sC_2(s)e^{s\beta y}\cos(sx)\,ds + c^{E}_{44}c_0, \tag{29}$$

$$D_{yi}(x,y) = -\frac{2d_{11}}{\pi}\int_0^\infty s[B_{1i}(s)e^{sy} - B_{2i}(s)e^{-sy}]\cos(sx)\,ds + d_{11}b_0, \tag{30}$$

$$\phi_i(x,y) = \frac{e_{15}}{d_{11}}\frac{2}{\pi}\int_0^\infty [A_{1i}(s)e^{s\alpha y} + A_{2i}(s)e^{-s\alpha y}]\cos(sx)\,ds + \frac{2}{\pi}\int_0^\infty [B_{1i}(s)e^{sy} + B_{2i}(s)e^{-sy}]\cos(sx)\,ds + \left(\frac{e_{15}}{d_{11}}a_0 - b_0\right)y, \tag{31}$$

$$E_{xi}(x,y) = \frac{e_{15}}{d_{11}}\frac{2}{\pi}\int_0^\infty s[A_{1i}(s)e^{s\alpha y} + A_{2i}(s)e^{-s\alpha y}]\sin(sx)\,ds + \frac{2}{\pi}\int_0^\infty s[B_{1i}(s)e^{sy} + B_{2i}(s)e^{-sy}]\sin(sx)\,ds. \tag{32}$$

By applying the far field and interface loading conditions, Eqs. (17)–(22), the constants a_0, b_0, c_0 and d_{0i} are evaluated as follows:

$$a_0 = \frac{d_{11}\tau_\infty + e_{15}D_0}{c_{44}d_{11} + e_{15}^2}, \quad b_0 = \frac{D_0}{d_{11}}, \quad c_0 = \frac{\tau_\infty}{c^{E}_{44}}, \quad d_{01} = (a_0 - c_0)h_1, \quad d_{02} = -(a_0 - c_0)h_2. \tag{33}$$

It is convenient to use the following definitions from Eqs. (15) and (16),

$$A_{11}(s) - A_{12}(s) \equiv D(s), \tag{34}$$

$$B_{11}(s) - B_{12}(s) \equiv E(s). \tag{35}$$

Using the two mixed boundary conditions Eqs. (10)–(14) with the aid of Eqs. (34) and (35), we obtain the following two simultaneous dual integral equations,

$$\int_0^\infty sf(s)D(s)\cos(sx)\,ds = \frac{\pi}{2}\frac{\tau_\infty}{\gamma}, \quad 0 \leqslant x < a, \tag{36}$$

$$\int_0^\infty D(s)\cos(sx)\,ds = 0, \quad a \leqslant x < \infty, \tag{37}$$

$$\int_0^\infty s\left[\frac{e_{15}}{d_{11}}D(s) + E(s)\right]\sin(sx)\,ds = 0, \quad 0 \leqslant x < a, \tag{38}$$

$$\int_0^\infty \left[\frac{e_{15}}{d_{11}}D(s) + E(s)\right]\cos(sx)\,ds = 0, \quad a \leqslant x < \infty, \tag{39}$$

where

$$f(s) = \frac{1}{\gamma}[(1+k^2)\alpha Q(s) - k^2 R(s)], \tag{40}$$

and

$$\gamma = \alpha + (\alpha - 1)k^2, \tag{41a}$$

$$Q(s) = \frac{[q_+(s) - q_-(s)\mathrm{e}^{-2s\alpha h_1}][q_+(s) - q_-(s)\mathrm{e}^{-2s\alpha h_2}]}{q_+^2(s) - q_-^2(s)\mathrm{e}^{-2s\alpha(h_1+h_2)}}, \tag{41b}$$

$$R(s) = \frac{(1-\mathrm{e}^{-2sh_1})(1-\mathrm{e}^{-2sh_2})}{1-\mathrm{e}^{-2s(h_1+h_2)}}, \tag{41c}$$

$$q_\pm(s) = c_{44}^*(1+k^2)\alpha \pm \beta, \quad c_{44}^* = c_{44}/c_{44}^{\mathrm{E}}, \tag{41d}$$

$$k = \sqrt{\mathrm{e}_{15}^2/c_{44}d_{11}}. \tag{41e}$$

It is readily seen from Eqs. (38) and (39) that

$$E(s) = -\frac{e_{15}}{d_{11}}D(s). \tag{42}$$

To solve Eqs. (36) and (37), let $D(s)$ be expressed by another function $\Omega(\xi)$ in the form

$$D(s) = \frac{\pi}{2}\frac{\tau_\infty a^2}{\gamma}\int_0^1 \sqrt{\xi}\Omega(\xi)J_0(sa\xi)\,\mathrm{d}\xi, \tag{43}$$

where $J_0(sa\xi)$ is the zero-order Bessel function of the first kind.

Upon substituting Eqs. (42) and (43) into Eqs. (36) and (37), we find that the auxiliary function $\Omega(\xi)$ is given by a Fredholm integral equation of the second kind in the form

$$\Omega(\xi) + \int_0^1 L(\xi,\eta)\Omega(\eta)\,\mathrm{d}\eta = \sqrt{\xi}, \tag{44}$$

where

$$L(\xi,\eta) = \sqrt{\xi\eta}\int_0^\infty s[f(s/a) - 1]J_0(s\eta)J_0(s\xi)\,\mathrm{d}s. \tag{45}$$

Eq. (44) is the governing integral equation for the current problem. Once the auxiliarly function $\Omega(\xi)$ is determined from Eq. (44), the entire electroelastic field is obtainable. Owing to the complicated form of the kernel, it seems unlikely that a closed form solution can be determined for $\Omega(\xi)$. However, the Fredholm integral Eq. (44) can be solved via some existing numerical schemes.

It is also easily seen that Eq. (44) is reduced to the corresponding static solution of Shin and Lee (2000) if we let $v = 0$. For the cases of $v = 0$ and $e = 0$, the present solution is reduced to the result of Narita et al. (1999). But the reduced solution is different from that of them, because of the error in their result (Kim and Lee, 2000).

3. Field intensity factors and energy release rate

Since of practical interest are the asymptotic fields near the crack tip, we can derive the asymptotic fields in the neighborhood of the propagating crack right as follows (Kwon and Lee, 2001):

$$\tau_{xz} = -\frac{K^{\mathrm{T}}(v)}{\gamma\sqrt{2\pi r}}\left[(1+k^2)\sqrt{\frac{r}{r_1}}\sin\left(\frac{\theta_1}{2}\right) - k^2\sin\left(\frac{\theta}{2}\right)\right], \tag{46}$$

$$\tau_{yz} = \frac{K^{\mathrm{T}}(v)}{\gamma\sqrt{2\pi r}}\left[(1+k^2)\alpha\sqrt{\frac{r}{r_1}}\cos\left(\frac{\theta_1}{2}\right) - k^2\cos\left(\frac{\theta}{2}\right)\right], \tag{47}$$

$$D_x = -\frac{K^{\mathrm{D}}(v)}{\sqrt{2\pi r}}\sin\left(\frac{\theta}{2}\right), \quad D_y = \frac{K^{\mathrm{D}}(v)}{\sqrt{2\pi r}}\cos\left(\frac{\theta}{2}\right), \tag{48}$$

where

$$r = \sqrt{(x-a)^2 + y^2}, \quad \theta = \tan^{-1}\left(\frac{y}{x-a}\right), \tag{49a}$$

$$r_1 = \sqrt{(x-a)^2 + (\alpha y)^2}, \quad \theta_1 = \tan^{-1}\left(\frac{\alpha y}{x-a}\right). \tag{49b}$$

Here $K^{\mathrm{T}}(v)$ and $K^{\mathrm{D}}(v)$ are the DSIF, and the dynamic electric displacement intensity factor (DEDIF), respectively. These field intensity factors are defined in the forms,

$$K^{\mathrm{T}}(v) = \lim_{x\to a^+}\sqrt{2\pi(x-a)}\tau_{yz}(x,0) = \tau_\infty\sqrt{\pi a}\Omega(1), \tag{50}$$

$$K^{\mathrm{D}}(v) = \lim_{x\to a^+}\sqrt{2\pi(x-a)}D_y(x,0) = \frac{e_{15}}{c_{44}\gamma}K^{\mathrm{T}}(v) = \frac{e_{15}\tau_\infty}{c_{44}\gamma}\sqrt{\pi a}\Omega(1). \tag{51}$$

By evaluating the DERR $G(v)$ suggested by Pak (1990) and Narita and Shindo (1998) with Eqs. (46)–(48), (49a), (49b), (50), (51) we obtain the following equations

$$G(v) = \frac{\mu\alpha[K^{\mathrm{T}}(v)]^2}{2(c_{44}\gamma)^2} - \frac{[K^{\mathrm{D}}(v)]^2}{2d_{11}} = \frac{[K^{\mathrm{T}}(v)]^2}{2c_{44}\gamma} = \frac{\tau_\infty^2\pi a}{2c_{44}\gamma}\Omega^2(1). \tag{52}$$

It is noted that the DERR can be expressed in terms of the DSIF and depends on the resultant stress distribution only generated by the mechanical deformation and the electromechanical interaction.

Chen and Yu (1997) presented that a Mach number, $M(=v/C_{\mathrm{T}})$, had no influence on both the DSIF and the DEDIF in an infinite piezoelectric material under the impermeable crack condition. Their solutions are

$$K_\infty^{\mathrm{T}}(v) = \tau_\infty\sqrt{\pi a}, \quad K_\infty^{\mathrm{D}}(v) = D_0\sqrt{\pi a}, \quad G_\infty(v) = \frac{\mu\alpha\tau_\infty^2\pi a}{2(c_{44}\gamma)^2} - \frac{D_0^2\pi a}{2d_{11}}. \tag{53}$$

Eq. (53) show that the DEDIF depends on the electric load, D_0, and the DERR is always negative under electric loading only, irrespective of its sign as like in a static problem.

The present solutions based on the permeable crack model can be easily degenerated to those of an infinite piezoelectric material by letting $h \to \infty$. In the case, the DSIF, DEDIF and DERR are given as follows:

$$K_\infty^{\mathrm{T}}(v) = \tau_\infty\sqrt{\pi a}, \quad K_\infty^{\mathrm{D}}(v) = \frac{e_{15}K_\infty^{\mathrm{T}}(v)}{c_{44}\gamma}, \quad G_\infty(v) = \frac{\tau_\infty^2\pi a}{2c_{44}\gamma}. \tag{54}$$

In the present results, it can be observed that the DSIF does not depend on crack speed as like in a purely elastic infinite material. On the while, it is noted that the DEDIF does not depend on electric loading but does depend on crack speed v, which is different from Eq. (53). If we consider mechanical terms only, viz. $e_{15} = 0$, Eq. (54) is exactly reduced to the purely elastic solutions of Freund (1990), but Eq. (53) is not.

On the other hand, when the geometry of the medium is such as the strip, the values of field intensity factors of Eqs. (50) and (51) are dependent on both the finite geometry and the crack propagation speed M.

4. Discussions

It is well known phenomenon that no anti-plane mode surface wave exists in the purely elastic solids, but piezoelectricity enables the existence of certain kinds of bound surface wave. This SH mode surface wave velocity (Bleustein, 1968) is defined as $v_s = C_T\sqrt{1-k_e^4}$, where $k_e = \sqrt{e_{15}^2/(d_{11}\mu)}$. The parameter k in Eq. (41e) is related to k_e in the form,

$$k = \frac{k_e}{\sqrt{1-k_e^2}}. \tag{55}$$

We call the parameter k as the EMCC.

The effects of the EMCC on the dimensionless DSIF and DERR are shown in Figs. 2 and 3. Fig. 2 displays $K^*(\equiv K^T(v)/\tau_\infty\sqrt{\pi a})$ versus M for three different EMCC k. The normalized DSIF K^* decreases or increases with the increase of EMCC as M increases, depending on the stiffness ratio $c_{44}^*(=c_{44}/c_{44}^E)\lesseqgtr 1$ between the piezoelectric material and the surrounding elastic materials.

Fig. 3 shows $G^*(\equiv G(v)/G_\infty(v=0))$ versus M. Here $G^* = \Omega^2(1)/\gamma$. The normalized DERR G^* always increases with increases of M, while it has lower value for higher value of EMCC in certain small M level, but the trend is reversed in higher M level.

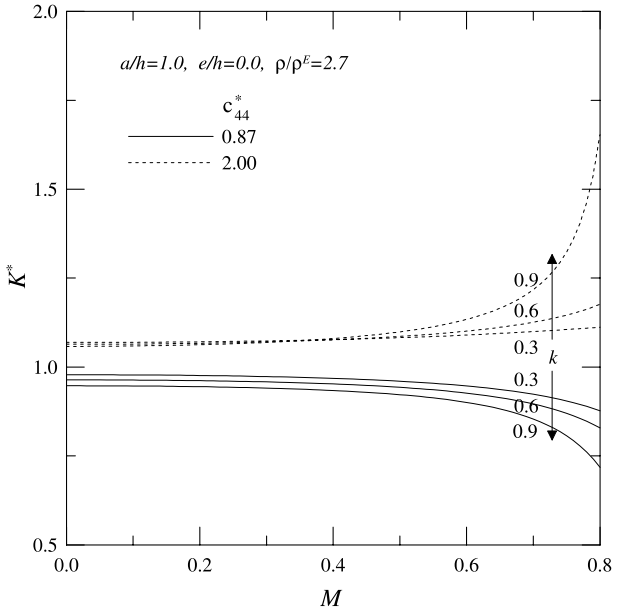

Fig. 2. K^* versus M for several different EMCC k.

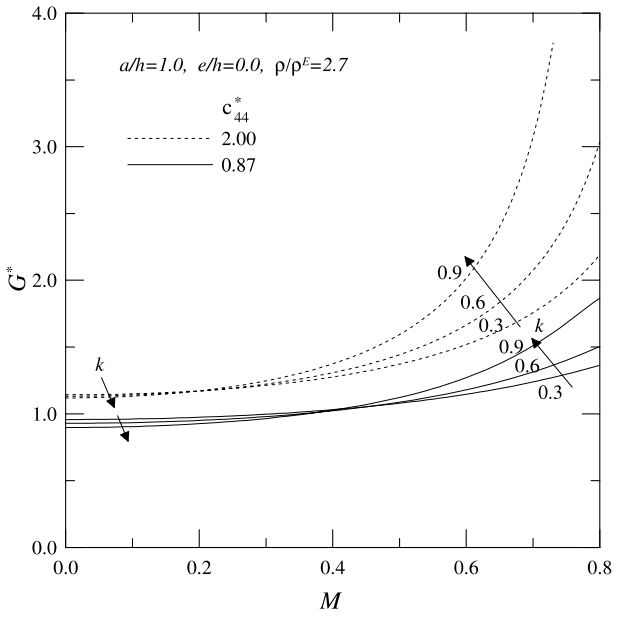

Fig. 3. G^* versus M for several different EMCC k.

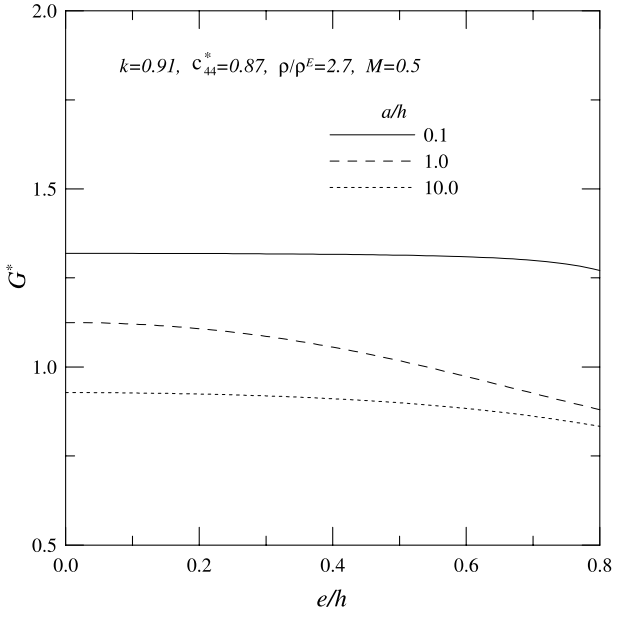

Fig. 4. G^* versus e/h.

Fig. 4 shows G^* versus e/h with the variations of $a/h = 0.1$, 1.0 and 10.0 for the cases of $k = 0.91$, $c_{44}^* = 0.87$, $\rho/\rho^{\mathrm{E}} = 2.7$ and $M = 0.5$. The corresponding material combination is Al/PZT-5H/Al structure (for the selected material properties, see Shin and Lee, 2000). The DERR G^* decreases with the increases of

e/h. It also shows that the higher value of a/h gives the lower value of G^*. But this trend is always not true as shown in the static results of Shin and Lee (2000). It depends on the material combinations, c_{44}^*.

To investigate the initial crack branching of the brittle electroelasticity, we use the criterion of maximum energy release rate. Using the polar coordinate system (r,θ) defined at the right of crack tip (Fig. 1), the field intensity factors along the orientation θ are

$$K^{\mathrm{T}}(v,\theta) = K^{\mathrm{T}}(v)\Theta(\theta), \quad K^{\mathrm{D}}(v,\theta) = K^{\mathrm{D}}(v)\cos\frac{\theta}{2}, \tag{56}$$

where

$$\Theta(\theta) = \frac{1}{\gamma}\left[(1+k^2)\alpha R(\theta)\cos\theta\cos\frac{\theta_1}{2} + (1+k^2)R(\theta)\sin\theta\sin\frac{\theta_1}{2} - k^2\cos\frac{\theta}{2}\right], \tag{57a}$$

$$R(\theta) = \sqrt{\frac{r}{r_1}} = \sqrt[4]{\frac{1+\tan^2\theta}{1+\alpha^2\tan^2\theta}}, \quad \tan\theta_1 = \alpha\tan\theta. \tag{57b}$$

Therefore, at the crack branching the DERR can be found in the form,

$$G(v,\theta) = \frac{\mu\alpha[K^{\mathrm{T}}(v,\theta)]^2}{2(c_{44}\gamma)^2} - \frac{[K^{\mathrm{D}}(v,\theta)]^2}{2d_{11}} = G(v)F(\theta), \tag{58}$$

where

$$F(\theta) = \frac{1}{\gamma}\left[(1+k^2)\alpha\Theta^2(\theta) - k^2\cos^2\frac{\theta}{2}\right]. \tag{59}$$

For numerical results of the initial crack branch, we consider PZT-5H piezoelectric ceramic. The relevant material properties (Pak, 1990) are $c_{44} = 3.53\times10^{10}$ N/m^2, $e_{15} = 17.0$ C/m^2, $d_{11} = 151\times10^{-10}$ C/V m. The critical Mach number, $M_{\mathrm{c}} = 0.36$, for PZT-5H ceramic is obtained by calculating the extreme values of $F(\theta)$. While at lower Mach numbers $M \leqslant M_{\mathrm{c}}$, $F(\theta)$ monotonically decreases with increase of θ (Fig. 5), the

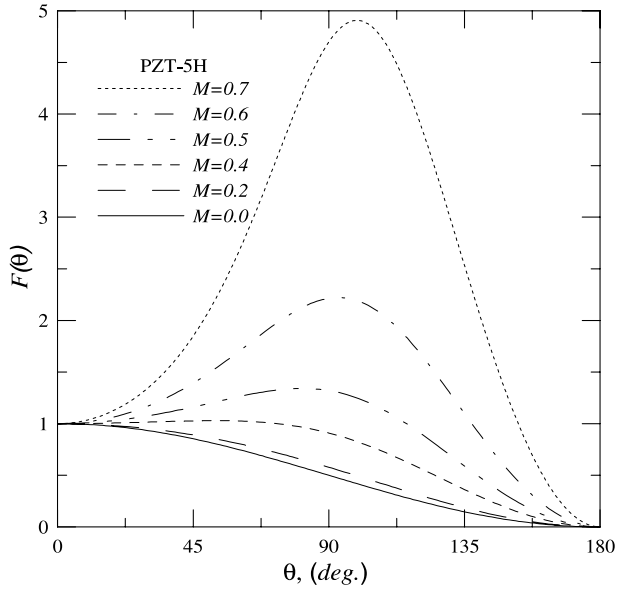

Fig. 5. $F(\theta)$ versus θ.

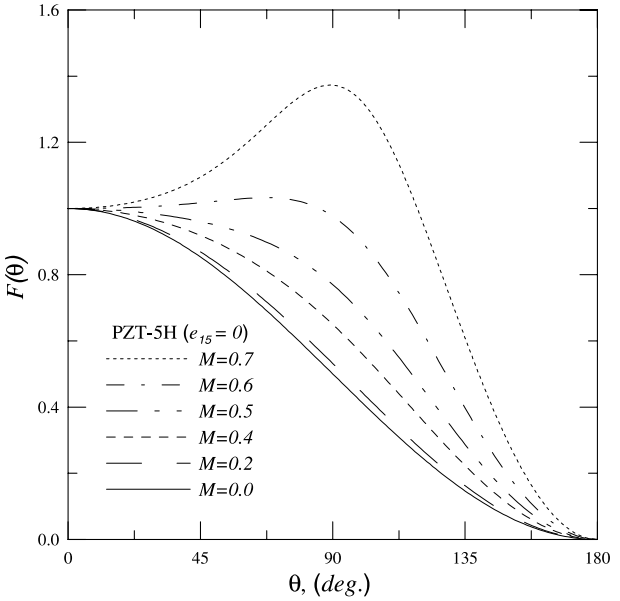

Fig. 6. $F(\theta)$ versus θ in case of $e_{15} = 0$.

maximum value of the DERR $G(v, \theta)$ occurs at the crack axis $\theta = 0$ and the direction of the crack growth is along the crack axis.

For the case of $M > M_c$, the function $F(\theta)$ increases with increase of θ at first and then decreases after it reaches a certain peak value. The angle θ_b corresponding to a peak value is the branch angle based on the criterion of maximum energy release rate. Furthermore, the higher crack propagation speed, the bigger branch angle. To show the effect of electrical loading, the $F(\theta)$ plot of the mechanical loading only without the electrical loading is shown in Fig. 6. It is evident from Figs. 5 and 6 that the bigger branch angles and the higher $F(\theta)$ values can be seen in presence of the electrical loading.

5. Conclusions

A Griffith eccentric crack moving at constant velocity in a transversely isotropic piezoelectric ceramic strip bonded to two elastic materials under combined anti-plane mechanical shear and in-plane electrical displacement loads is analyzed by the permeable crack model and the integral transform approach. The traditional concept of linear elastic fracture mechanics is extended to include the piezoelectric effects and the results are expressed in terms of the field intensity factors and the DERR. One can confirm that the EMCC and the stiffness ratio (c_{44}^*) are key parameters in the behaviors of piezoelectric composites. For the case of the piezoelectric material with the surrounding geometries, the crack propagation speed have influences on the DSIF and DERR. The kinetic energy of the crack moving at the high speed can change the propagation orientation of the moving crack.

References

Bleustein, J.L., 1968. A new surface wave in piezoelectric materials. Applied Physics Letters 13, 412–413.

Chen, Z.T., Karihaloo, B.L., Yu, S.W., 1998. A Griffith crack moving along the interface of two dissimilar piezoelectric materials. International Journal of Fracture 91, 197–203.

Chen, Z.T., Yu, S.W., 1997. Antiplane Yoffe crack problem in piezoelectric materials. International Journal of Fracture 84, L41–L45.
Freund, L.B., 1990. Dynamic Fracture Mechanics. Cambridge Press, Cambridge.
Jackson, J.D., 1976. Classical electrodynamics. John Wiley and Sons, New York.
Kim, K.Y., Lee, K.Y., 2000. A comment on anti-plane shear crack in a piezoelectric layer bonded to dissimilar half spaces. JSME International Journal Series A 43 (2), 196–197.
Kwon, S.M., Lee, K.Y., 2001. Constant moving crack in a piezoelectric block: anti-plane problem. Mechanics of Materials 33, 649–657.
Narita, F., Shindo, Y., 1998. Dynamic anti-plane shear of a cracked piezoelectric ceramic. Theoretical and Applied Fracture Mechanics 29, 169–180.
Narita, F., Shindo, Y., Watanabe, K., 1999. Anti-plane shear crack in a piezoelectric layer bonded to dissimilar half spaces. JSME International Journal Series A 42 (1), 66–72.
Pak, Y.E., 1990. Crack extension force in a piezoelectric materials. Transactions of ASME, Journal of Applied Mechanics 57, 647–653.
Park, S.B., Sun, C.T., 1995a. Effect of electric field on fracture of piezoelectric ceramics. International Journal of Fracture 70, 203–216.
Park, S.B., Sun, C.T., 1995b. Fracture criteria for piezoelectric ceramics. Journal of the American Ceramic Society 78, 1475–1480.
Shin, J.W., Lee, K.Y., 2000. Eccentric crack in a piezoelectric strip bonded to half planes. European Journal of Mechanics A/Solids 19, 989–997.
Tobin, A.G., Pak, Y.E., 1993. Effect of electric field on fracture behavior of PZT ceramics. Proceedings of SPIE, Smart Structures and Materials 1916, 78–86.
Yoffe, E.H., 1951. The moving Griffith crack. Philosophical Magazine 42, 739–750.